The International Journal of Advanced Manufacturing Technology (2018) 97:857–865
https://doi.org/10.1007/s00170-018-1981-2

ORIGINAL ARTICLE

Influence of machining parameters and tool structure on cutting force and hole wall damage in drilling CFRP with stepped drills

Xinyi Qiu[1] · Pengnan Li[1] · Qiulin Niu[1] · Anhua Chen[2] · Puren Ouyang[1] · Changping Li[1] · Tae Jo Ko[3]

Received: 7 September 2017 / Accepted: 2 April 2018 / Published online: 13 April 2018

Abstract
Carbon fiber-reinforced plastics (CFRPs) have many excellent properties, such as lightless, high specific strength, and high corrosion resistance, and they have been extensively used in the aeronautics and astronautics. It is a challenge for studies on the defect-free drilling technology and the causes of drilling defects to the CFRP materials. The purpose of this study is to research the machining parameters and the stepped drill geometry effect on cutting force and hole wall damage with the test methods. Both a twist drill and three stepped drills were employed in drilling CFRP plates under the experimental conditions. The effects of both the processing parameters and the stepped drill structure (the ratio of the pilot section diameter to the sizing diameter section diameter (D_1/D)) on thrust force and hole wall damage were investigated, and the damage mechanism of hole walls was revealed by analyzing the cross-section features of the hole wall. The results show that the maximum thrust force of T3 ($D_1/D = 0.5$) is minimal, so T3 should be selected to reduce the risk of delamination. D_1/D, feed rate, and spindle speed are the main factors that affect the size of the hole wall damage. In addition, a special cutting force F_{spec} is defined to explain the influence of tool structure and feed rate on hole wall damage.

Keywords CFRP · Drilling force · Hole wall damage · Stepped drill

1 Introduction

With the excellent high strength-to-weight ratio, high stiffness-to-weight ratio, and high corrosion resistance, carbon fiber-reinforced plastics have a wide range of applications in aerospace and defense [1, 2].

Drilling is one of the most important processing methods of machining CFRP, and usually is the final operation for the aerostructures's assembly. The hole quality usually affects both the assembly quality and the service life of the aircraft. The current situation is that the CFRP material is an anisotropic material, and its processing mechanisms are different from metal. The cutting surface of CFRP produces a lot of unique features [3], such as cracks, burrs, fiber pull out, and delamination. These unique features are easily affected by processing parameters, tool geometry, tool types, and materials. In addition, these features will weaken the part structure and the assembly quality.

Many scholars have done a lot of researches on the problem of drilling CFRP. Thrust force is the main cause of serious delamination. Both processing parameters and tool geometry are the major factors affecting thrust force. The maximum thrust force was drastically affected by the machining parameters [4]. Krishnaraj et al. [5] studied the impacts of the cutting parameters on the machinability of T300 woven CFRP laminates under the condition of high-speed drilling, and the results showed that the feed rate had a great influence on thrust force, push-out delamination, and diameter of the hole than the spindle speed. The delamination factors increased with the increase of the feed rate or the spindle speed. To reduce the thrust force and the delamination, Schulze et al. [6] recommended setting the feed at low values, especially in the drilling process of UD-CFRP. Lazar et al. [7] studied the effects of machining parameters and drill geometries on cutting forces. They presented the force distributions along the cutting edges

✉ Pengnan Li
2002lpn@163.com

[1] College of Mechanical and Electrical Engineering, Hunan University of Science and Technology, Xiangtan, China

[2] Hunan Provincial Key Laboratory of Health Maintenance for Mechanical Equipment, Hunan University of Science and Technology, Xiangtan, China

[3] School of Mechanical Engineering, Yeungnam University, Gyeoungsan, South Korea

at low feed and also showed that the feed and the drill geometry both were the most important parameters.

The tool structure, material, and type have been extensively researched [8, 9]. One type of the twist drill and one type of the drill with special geometry were used for drilling the thin carbon/epoxy laminates by Piquet et al. [10]. They summarized that the smaller contact length between the special geometry drill and the hole might result in less delamination. Xu et al. [11] carried a study on drilling of T800S/250F CFRP laminates with two kinds of drills: a dagger drill and a twist drill. The results showed that increasing the thrust force would result in exacerbating delamination damage greatly, and the dagger drill gave better drilling performance than the twist drill. Shyha et al. [12] found that when an uncoated WC stepped drill was used at higher feed rate (0.2 mm/rev rather than 0.1 mm/rev) it could significantly increase the number of holes made productivity (up to 50% improvement). Tsao and Hocheng [13, 14] studied the influence on the delamination factor by using various type drills: twist drill, candle stick drill, and saw drill. Analytically, they predicted the various drill bits thrust force, and compared with a twist drill. To study the impact of the drill geometry on unidirectional laminate GFRPs, Bhatnagar et al. [15, 16] carried out a comparative study. The results indicated that eight facet and Jo-drills were suitable drills for drilling composite materials duo to the lower thrust force and torque. Karpat et al. [17–19] and Wang et al. [20] drilled the CFRP with double point angle drills. They suggested that the workpiece properties, tool geometry, and processing conditions must be taken into consideration in the selection of process parameters. To research the effect of drill bit geometry on the thrust force, Durao et al. drilled the GFRP and CFRP composite laminates with various drill bit geometries, and the results showed that the brad point drill bits and step drill bits produced lower thrust force than the standard twist drill and slot drill while drilling composite laminates [21–24]. The conventional twist drills with diameters of 8, 9, 10, 11, 12, and 13 mm were used to study the influence of the drill diameter on the thrust force and torque [25]. The results showed that thrust force and torque increased with drill diameter and feed rate. Mohan et al. also studied the influence of drill diameters and feed rate on thrust force and torque [26]. Teti emphasized the importance to develop better drill structures and processing strategies [27].

Currently, research on machining CFRP mainly focuses on the superficial phenomenon of the cutting force, matrix

breakage, and fiber breakage [28], but pays little attention on hole wall damage in the process of UD-CFRP drilling and lacks the work of the deeper damage mechanism. A pilot hole forms after the primary stage of the stepped drill drilling, which can reduce the threat to delamination significantly and obtain a larger critical thrust force at the beginning of delamination [29]. Also, increasing the critical thrust force, larger processing parameters can be chosen, which can improve processing efficiency. Therefore, with the application of a stepped drill, a reduction in energy consumption can be expected, which is meaningful for green manufacturing. Taguchi method and radial basis function network were used to predict the thrust force of stepped drill [30]. However, few research on drilling CFRP unidirectional plates with stepped drill has been reported, and little attention has been paid on the geometry of the stepped drill on the thrust force and the hole wall damage. The purpose of this study is to research the machining parameters and the stepped drill geometry effect on cutting force and hole wall damage, to provide a reference for the hole wall damage controlling and tool design in the process of composite laminates drilling. A twist drill and three stepped drills are employed in drilling CFRP plates under the experimental conditions. The effects of the processing parameters and the drill geometrical structure on thrust force and hole wall damage are investigated, and the damage mechanism of the hole wall is analyzed.

2 Test conditions

The workpiece is a unidirectional CFRP plate with a thickness of 4.9 mm. Figure 1 shows the schematic of CFRP structure. The reinforcing fiber is Toaray-T800S, and the epoxy matrix is Toray 250F. All fibers are in the same direction (see Fig. 1).

The drills are made of ultra-fine grain carbide bars with the identical diameter of 6 mm. T1 is an uncoated twist drill. T2, T3, and T4 are uncoated twin lipped stepped drills, incorporating a 6-mm sizing diameter section with a pilot diameter of 4.5, 3, and 2 mm, respectively. The drill morphology is shown in Fig. 2. Both stepped drill schematic and the geometric parameters of the used drill bits were displayed in Fig. 3 and Table 1, respectively.

Experiments are conducted on a KVC800/1 Vertical Machining Center. The spindle speed range is 0–6000 rev/min. The full factor experiment including 15 cutting parameters is designed (spindle speed (n) 1500, 3500, and 5500 rev/min, feed rate (f) 0.01, 0.02, 0.03, 0.04, 0.05 mm/rev), and all tests are performed under a dry condition. The test conditions are shown in Table 2.

The cutting force was measured using a Kistler 9253B23 force dynamometer and a Kistler 5080A charge amplifier. The force signals are sampled with a 32-bit PC-based data

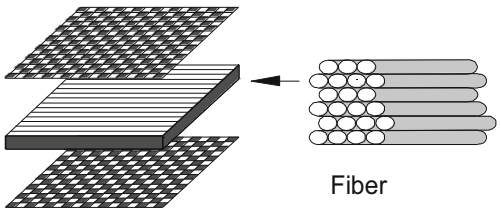

Fig. 1 The schematic of CFRP structure

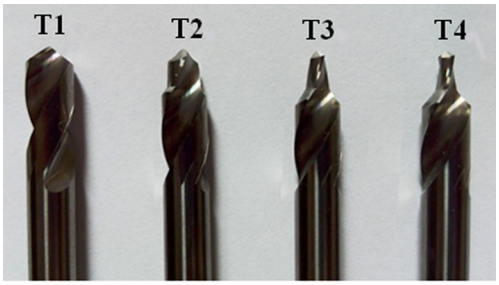

Fig. 2 Drill geometries (T1) twist drill, (T2–4) stepped drill

acquisition system. Scanning electron microscopy (JMS-6308LV) is used to observe the hole wall surface morphology.

3 Results and discussions

3.1 Drilling force

For drilling polymer matrix composites, the thrust force is the main reason for delamination. Figure 4 shows a typical thrust force plot of the stepped drill. The 1–4 stages are twist drill drilling process. In the 1–2 stages, with the cutting edge cutting into the workpiece material, the thrust force is increased from zero. When all the cutting edges are involved in the drilling, the thrust force increases to its peak (for stepped drill that is the first peak.). In the 2–3 stages, drill tip, chisel edge, and main cutting edge are cutting into the workpiece material, which causes a reducing of the distance between the chisel edge and bottom of the workpiece. So, the workpiece material reduces the tool support stiffness, leading a reduction in the drilling thrust. In the 3–4 stages, as the drilling proceeds, the drill tip firstly cut off the workpiece bottom and the chisel edge is not involved in cutting. Therefore, the thrust force is reduced. If a twist drill is used, the thrust force will reduce to zero in this stage. The next 4–7 stages are the unique stages of the stepped drill. The 4–5 stages are similar to the 1–2 stages. However, only the main cutting edges (sizing diameter section of the stepped drill) gradually cut into the workpiece material. When all the cutting edges involve in the drilling, the axial thrust increases to its second peak. The 5–6 stage is similar to the 2–3 stages. In the 6–7 stage, the main cutting edge of the sizing diameter section is the only cutting edge. The thrust force trend is similar to the 3–4 stages. In the 7–8 stages, the main cutting edge (sizing diameter section of the stepped drill) firstly cuts off the workpiece bottom and the thrust force reduces to zero.

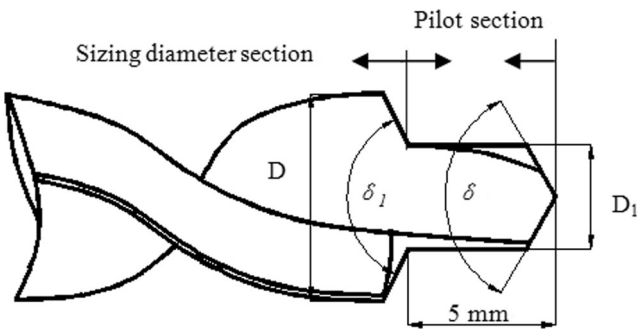

Fig. 3 Stepped drill schematic

Table 1 Geometric parameters of the used drill bits

Tool type	D (mm)	D_1/D	δ_1 (°)	Point angle δ (°)	Helix angle β (°)
T1	6	1	–	110	28
T2	6	0.75	90	110	28
T3	6	0.5	90	110	28
T4	6	0.33	90	110	28

Figure 5a shows the thrust force for these four tools at n = 3500 rev/min and f = 0.03 mm/rev, and Fig. 5b shows the torque for tools at n = 3500 rev/min and f = 0.03 mm/rev. The maximum thrust forces are different due to the different tool structures. When drilling with the stepped drill, the thrust force appears two peaks: one is at point 2 (see Fig. 4), and the other is at point 5 (see Fig. 4). The maximum thrust force of the twist drill T1 appears at the point 2 (see Fig. 4). The two thrust force peaks of the stepped drill T2 are almost equally, but the maximum thrust force of the stepped drill T3 and T4 appear at the point 5 (see Fig. 4). The maximum thrust forces of T2, T3, and T4 are 25.93, 41.55, and 33.72% less than T1, respectively. The maximum torques of T2, T3, and T4 are 33.55, 52.72, and 50.48% less than T1, respectively.

As can be seen from Fig. 6, the thrust forces of the four drills increase dramatically as the feed rate is elevated. This is mainly because the elevated feed rate leads to an increasing in cutting depth per revolution, and the drill bit is required to cut off more material volumes per revolution and to overcome much high drilling resistance. So, the thrust forces increase.

Table 2 Test conditions

Workpiece	
Reinforcing	Toaray-T800S
Epoxy matrix	Toray 250F
Fiber volume content	60%
Fiber bundle	5 μm, 24 K
Thickness	4.9 mm
Drill	
Material	Ultra-fine grain carbide
Diameter	6 mm
Type	Stepped drill
Machining parameters	
Spindle rotation (n)	1500, 3500, 5500 rev/min
Feed rate (f)	0.01, 0.02, 0.03, 0.04, 0.05 mm/rev

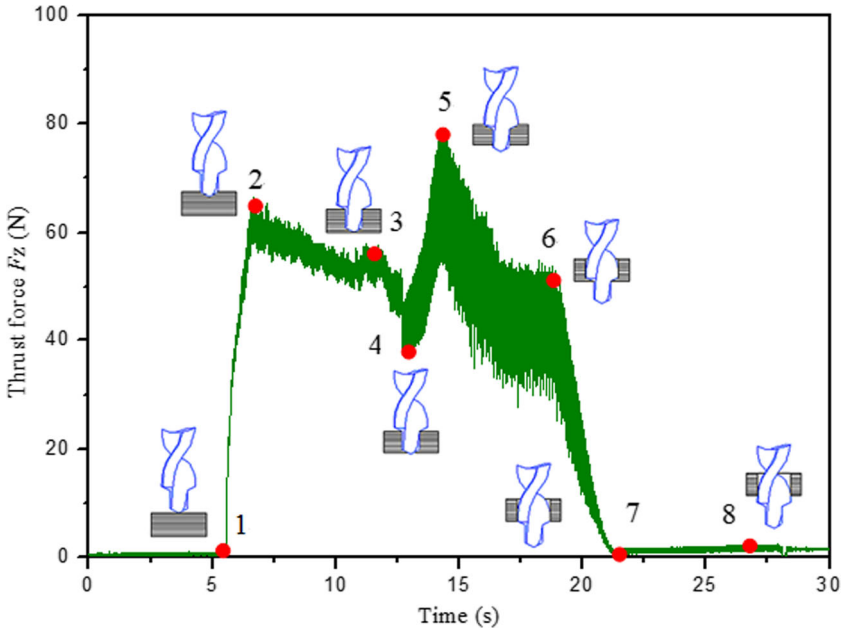

Fig. 4 A typical thrust force plot of the stepped drill

As shown in Fig. 6, it is noted that the variation of the maximum thrust forces is small under different spindle speeds. The gap among the maximum thrust forces at $n = 1500$ rev/min and $n = 5500$ rev/mm is less than 10 N. Therefore, the feed rate is the main factor affecting the thrust force. This conclusion is in agreement with the Ref. [11].

It can be found from Fig. 7 that the maximum thrust forces firstly decrease with the increasing of the D_1/D and reach a valley value at D_1/D of 0.5. Then, it increases with D_1/D. Under the same processing conditions, the maximum thrust forces of the twist drill (T1) are bigger than the stepped drills (T2, T4, and T3). The main reason is that the stepped drill drills the pilot holes first, and then expands the pilot hole to the sizing diameter. Therefore, the influence of the chisel edge on the thrust force has been eliminated, resulting in a reducing on the maximum thrust force. When the ratio of D_1/D of the stepped drill is 0.75, the two peaks of the thrust force are almost equal. Therefore, it can conclude that the chisel edge has no contribution to the maximum thrust force when the value of D_1/D is lower than 0.75.

The thrust forces produced by T2, T3, and T4 are 18–26, 33–46, and 24–33% less than T1, respectively. Here, the gap among the thrust forces is caused by the difference of the tool geometry. The maximum thrust force of T3 is minimal. So, in order to reduce the risk of delamination during the drilling process, T3 should be selected.

3.2 Hole wall surface morphology

The fiber cutting angle θ is defined as the angle between fiber orientation and cutting speed direction. Figure 8 shows the damage area of the hole wall that the hole drilled by T2 at $n = 1500$ rev/min and $f = 0.02$ mm/rev. Figure 8e, f, g corresponds to the position A, B, and C at Fig. 8b, respectively. For $\theta = 0$~90°, the machined surface shows better quality than that

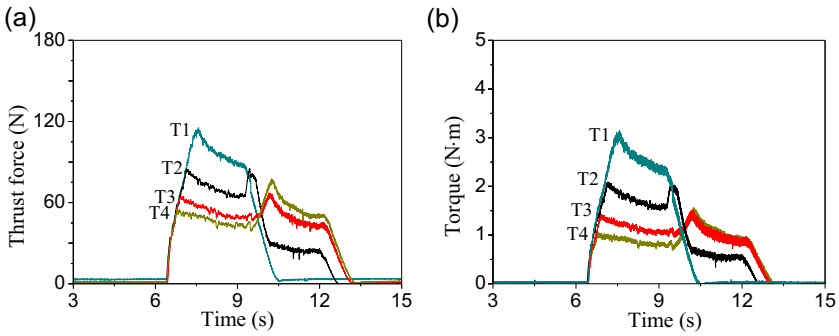

Fig. 5 **a** Thrust force. **b** Torque. ($n = 3500$ rev/min and $f = 0.03$ mm/rev)

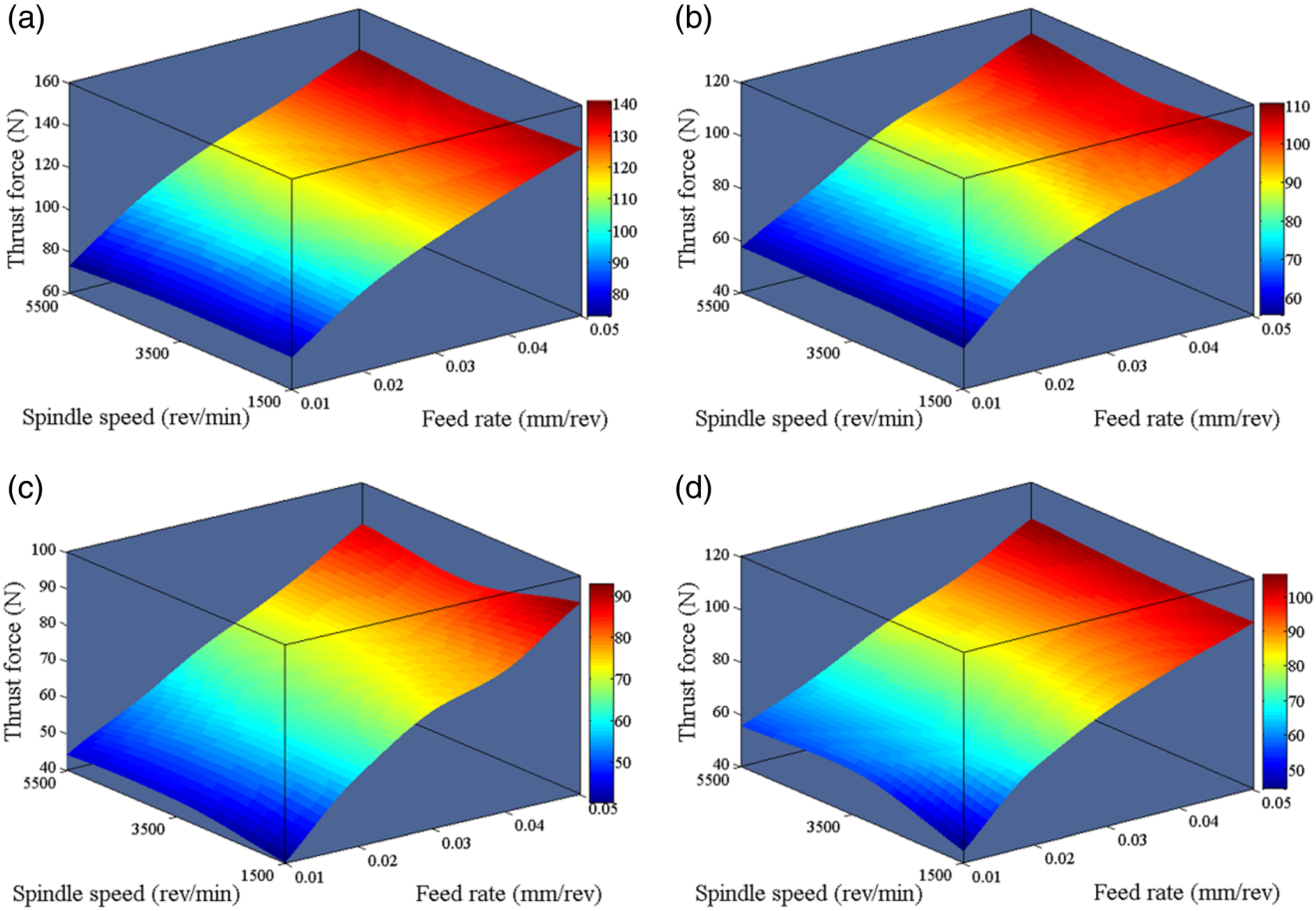

Fig. 6 Maximum thrust force in function for different tools (**a** T1, **b** T2, **c** T3, **d** T4)

of $\theta = 90°\sim180°$. s is defined as the area of the hole wall damage (see Fig. 8b).

Figure 9 shows the cross-section features of the hole wall. The damage area distribute at the hole wall where θ is 120°~150°. In the damage area, the degree of damage weakened along the direction of the tool rotation. The most serious degree of overcut damage appears at $\theta = 150°$ (see Fig. 8g). Then the overcut damage weakens at $\theta = 135°$ (Fig. 8f), finally disappears at $\theta = 120°$ (see Fig. 8e). h is defined as the depth of the hole wall damage (see Fig. 9), and the range of h is 60–95 μm measured in the experiments.

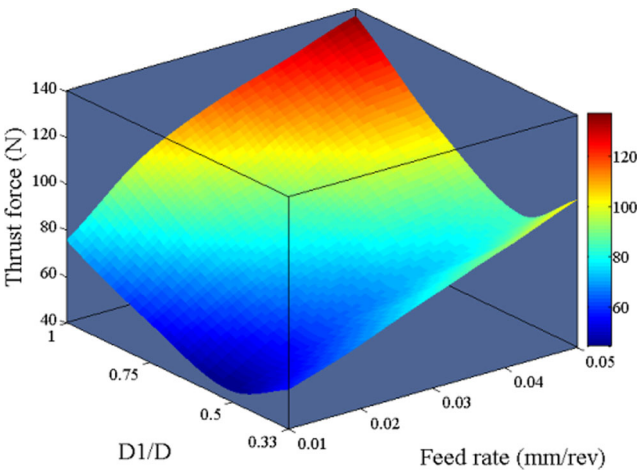

Fig. 7 Maximum thrust force in function for D_1/D ($n = 3500$ rev/min)

When θ is in the range of 90°~180°, the fibers breaking occurs by the maximum bending stress. So the breaking point is not at the cutting edge but at the bottom of the cutting edge, and that means the fiber bundles are broken. Thus, some materials under the bottom of the cutting edge have been cut away, leading to a rough surface (see Fig. 8e–g). However, when $\theta = 0°\sim90°$, the fiber breaks under the shear and stretched action of the cutting edge, resulting in a high quality of hole wall surface.

Figure 10 shows the schematic of the damage formation of the hole wall. For the fiber cutting angle $\theta = 90°\sim180°$,

$$F_2 = F_s \times \cos(\theta - 60) \quad (1)$$

When the tool rotates from H_1 to H_2, θ changes from 180° to 90°, leading to an increase in F_2. When F_2

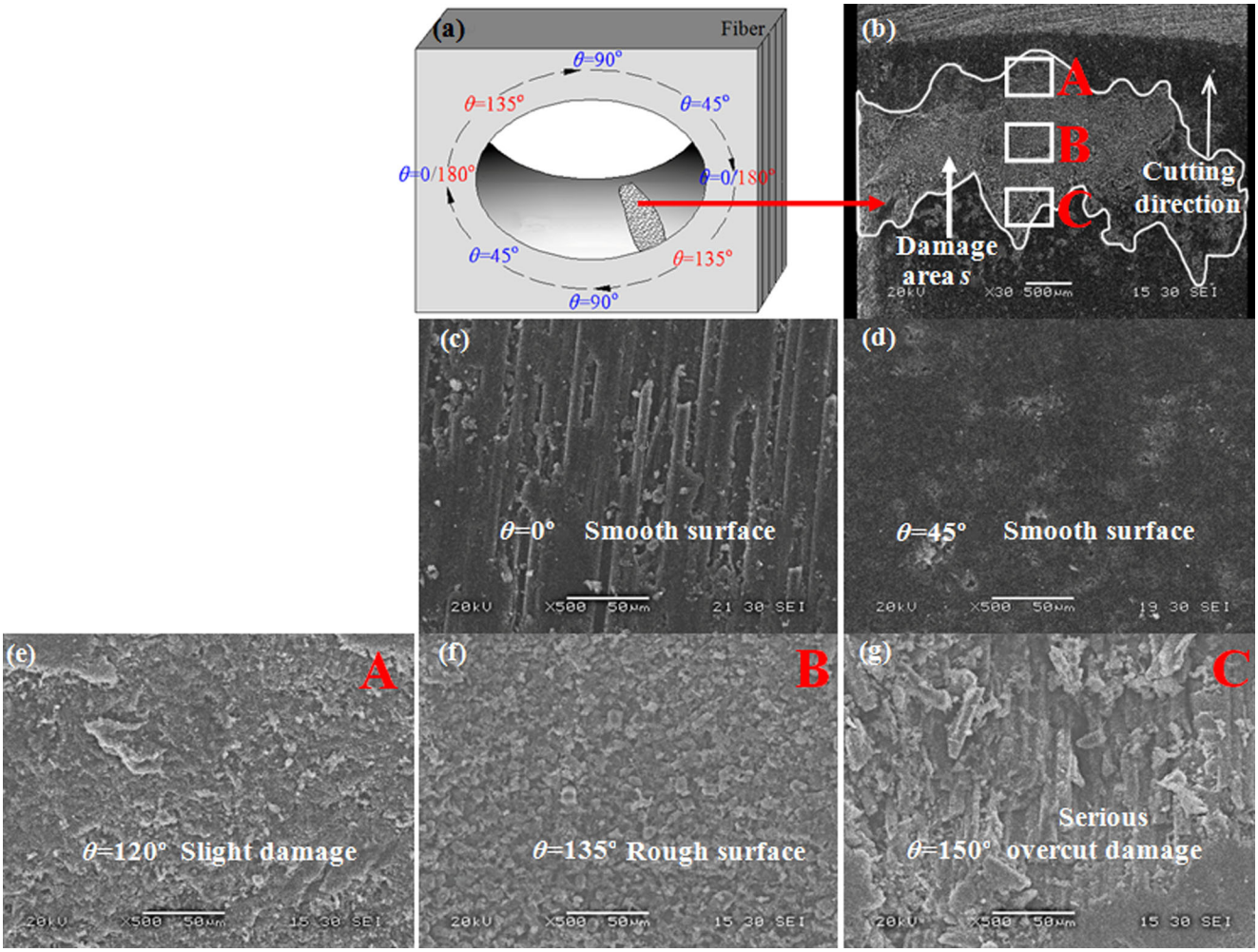

Fig. 8 **a** The schematic of the hole wall damage. **b** Hole wall damage morphology. **c** $\theta = 0°$. **d** $\theta = 45°$. **e** Position A. **f** Position B. **g** Position C

reaches a certain value, the fibers have been torn and the damage of the wall surface occurs.

For the cutting edge moving from A to B, suppose that the number of carbon fibers which are cut off at position A is equal to those at position B, namely $S_1 = S_2$. Therefore, h_1 is greater than h_2, leading to a weakness phenomenon of the damage degree along the direction of rotation.

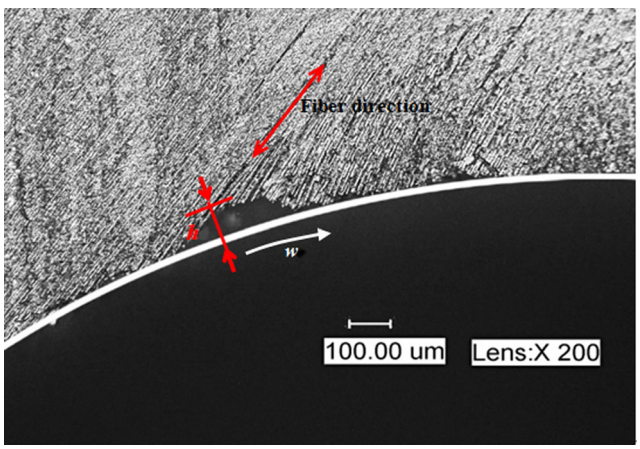

Fig. 9 The cross-section features of the hole wall for T2 ($n = 1500$ rev/min, $f = 0.01$ mm/rev)

3.2.1 Tool structure

Figure 11 shows the damage area s of the hole wall varies with feed rate for different spindle speeds. It shows that the damage area of T1 is biggest, and the damage area of T3 and T4 are relatively small at $n =$ 1500 rev/min. At $n = 5500$ rev/min, the damage area of T1 is almost equivalent to T3 and T4, while the damage area of T2 is the largest. The reason is that the remaining material in the hole wall is less (0.75 mm) after pilot section of T2. Therefore, the remaining material lacked restraint in sizing diameter section, resulting in larger damage. The order of the damage size of the hole wall of the stepped drill is T2 > T3 > T4. That is, it decreases as the ratio of D_1/D decreases. The hole wall is formed by the twist drill outer corner (the stepped

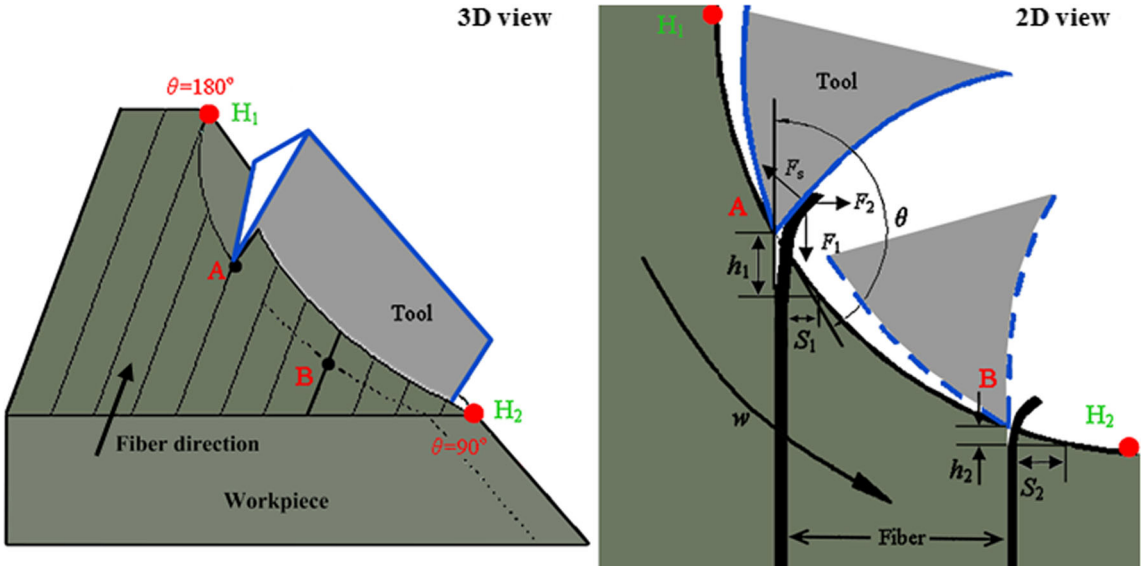

Fig. 10 The schematic of the damage formation of the hole wall

drill outer corner of the sizing diameter section), corresponding to the 5–6 stages in Fig. 4.

To explain the order of the damage areas T2 > T3 > T4, an analysis is reported as follows. Figure 12 shows the force diagram of a stepped drill at the 5–6 stages where F_{z1} is a projection of F_1.

$$F_z = 2F_{z1} \tag{2}$$

F_z is the average thrust force of the 5–6 stages.

Define a special cutting force:

$$F_{\text{spec}} = F_{z1}/(b \times f) \tag{3}$$

where b is sizing diameter section cutting width (see Fig. 12).

Figure 13 shows the curves of the special cutting force F_{spec} among the stepped drills. It can find the order of the special cutting force of the stepped drills is T2 > T3 > T4. Therefore, there is a positive correlation between the damage area and the special cutting force.

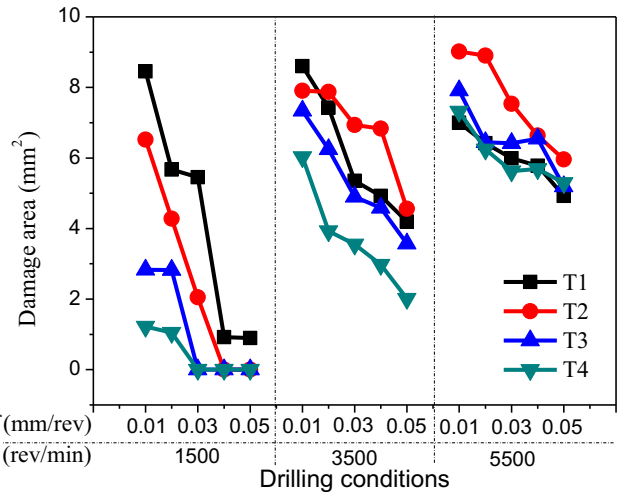

Fig. 11 The curves of damage area s for four drills at different spindle speeds

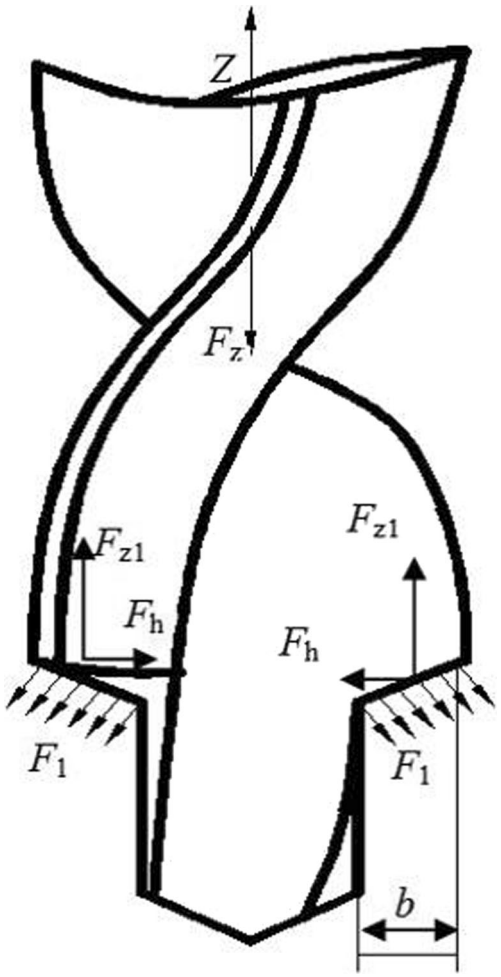

Fig. 12 The diagram of the force of a stepped drill at the 5–6 stages

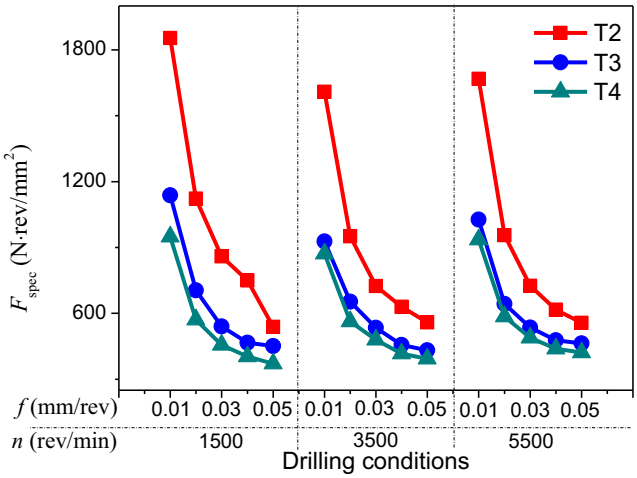

Fig. 13 The curves of the special cutting force F_{spec} of the stepped drills

3.2.2 Feed rate and spindle speed

Figure 11 also shows that the damage area decreases as the feed rate increases under the same spindle speed. Simultaneously, the special cutting force decreases with the increase of the feed rate (see Fig. 13). Therefore, the damage area decreases as the feed rate increases. The reason is that the elevated feed rate leads to an increase of the cutting depth per revolution, and the drill bit is needed to cut off more material volumes per revolution and to break more fibers. Therefore, the ratio of the thrust force to the number of fibers is reduced, resulting in a reduction of the damage area.

As shown in Fig. 11, it also shows that the damage area increases as the spindle speed increases at the same feed rate. In Wang's research, it reported that the temperature increases with the increase of the spindle speed [20]. The high temperature will soften the matrix material, leading to an increase of the damage area.

4 Conclusions

A twist drill and three stepped drills are employed in drilling CFRP plates under the experimental conditions. The effects of the processing parameters and the ratios of D_1/D on cutting force and hole wall damage are investigated, and the damage mechanism of hole wall is analyzed.

(1) The stepped drill shows better drilling performance than the twist drill, i.e., smaller maximum thrust force and hole wall damage area. The maximum thrust force of T3 is minimal. So, in order to reduce the risk of delamination and achieve high-quality hole wall during the drilling process, T3 should be selected.

(2) The maximum thrust force decreases first and then increases with D_1/D, and the valley appears at $D_1/D = 0.5$.

(3) The area of damage distributes at the hole wall where θ is in the range of 90°~180°. In the damaged area, the degree of damage weakened along the direction of the tool rotation.

(4) D_1/D, feed rate, and spindle speed are the main factors that affect the size of the hole wall damage. The damage area decreases as the feed rate increases, but it increases as the spindle speed increases.

Funding information The work is supported by the National Natural Science Foundation of China (No.51775184, No.51275168, No.51605161) and by the Hunan provincial Natural Science Foundation of China (No.2015JJ5028).

References

1. Wang HW, Sun J, Li JF, Li WD (2014) Investigation on delamination morphology during drilling composite laminates. Int J Adv Manuf Technol 74:257–266
2. Chen LX, Zhang KF, Cheng H, Qi ZC, Meng QX (2017) A cutting force predicting model in orthogonal machining of unidirectional CFRP for entire range of fiber orientation. Int J Adv Manuf Technol 89:833–846
3. Mishra R, Malik J, Singh I, Davim JP (2010) Neural network approach for estimate the residual tensile strength after drilling in unidirectional glass fiber reinforced plastic laminates. Mater Des 31:2790–2795
4. Su F, Wang ZH, Yuan JT, Cheng Y (2014) Study of thrust forces and delamination in drilling carbon-reinforced plastics (CFRPs) using a tapered drill-reamer. Int J Adv Manuf Technol 80:1457–1469
5. Krishnaraj V, Prabukarthi A, Ramanathan A, Elanghovan N, Kumar MS, Zitoune R, Davim JP (2012) Optimization of machining parameters at high speed drilling of carbon fiber reinforced plastic (CFRP) laminates. Compos Part B Eng 43:1791–1799
6. Schulze V, Becke C, Weidenmann K, Dietrich S (2010) Machining strategies for hole making in composites with minimal workpiece damage by directing the process forces inwards. J Mater Process Technol 211:329–338
7. Lazar MB, Xirouchakis P (2011) Experimental analysis of drilling fiber rein-forced composites. Int J Mach Tools Manuf 51:937–946
8. Anand RS, Patra K, Stiner M (2014) Size effects in micro drilling of carbon fiber reinforced plastic composite. Prod Eng Res Dev 8:301–307
9. Lau WS, Yue TM, Lee TC, Lee WB (1995) Un-conventional machining of composite materials. J Mater Process Technol 48:199–205
10. Piquet R, Ferret B, Lachaud F, Swider P (2000) Experimental analysis of drilling damage in thin carbon/epoxy plate using special drills. Compos Part A Eng 31:1107–1115
11. Xu JY, An QL, Cai XJ, Chen M (2013) Drilling machinability evaluation on new developed high-strength T800S/250F CFRP laminates. Int J Precis Eng Manuf 14:1687–1696
12. Shyha IS, Aspinwall DK, Soo SL, Bradley S (2009) Drill geometry and operating effects when cutting small diameter holes in CFRP. Int J Mach Tools Manuf 49:1008–1014
13. Tsao CC, Hocheng H (2004) Taguchi analysis of delamination associated with various drill bits in drilling of composite material. Int J Mach Tools Manuf 44:1085–1090

14. Tsao CC, Hocheng H (2005) Effect of eccentricity of twist drill and candle stick drill on delamination in drilling composite materials. Int J Mach Tools Manuf 45:125–130
15. Bhatnagar N, Singh I, Nayak D (2004) Damage investigation in drilling of glass fiber reinforced plastic composite laminates. Mater Manuf Process 19:995–1007
16. Singh I, Bhatnagar N (2006) Drilling of uni-directional glass fiber reinforced plastic (UD-GFRP) composite laminates. Int J Adv Manuf Technol 26:870–876
17. Karpat Y, Değer B, Bahtiyar O (2012) Drilling thick fabric woven CFRP laminates with double point angle drills. J Mater Process Technol 212:2117–2127
18. Karpat Y, Değer B, Bahtiyar O (2014) Experimental evaluation of polycrystalline diamond tool geometries while drilling carbon fiber-reinforced plastics. Int J Adv Manuf Technol 71:1295–1307
19. Karpat Y, Bahtiyar O (2015) Tool geometry based prediction of critical thrust force while drilling carbon fiber reinforced polymers. Adv Manuf 3:300–308
20. Wang CY, Chen YH, An QL, Cai XJ, Ming WW, Chen M (2015) Drilling temperature and hole quality in drilling of CFRP/aluminum stacks using diamond coated drill. Int J Precis Eng Manuf 16:1689–1697
21. Durao LMP, Goncalves DJS, Tavares JMRS, de Albuquerque VHC, Aguiar Vieira A, Tomes Marques A (2010) Drilling tool geometry evaluation for reinforced composite laminates. Compos Struct 92:1545–1550
22. Abrao AM, Rubio JCC, Faria PE, Davim JP (2008) The effect of cutting tool geometry on thrust force and delamination when drilling glass fiber reinforced plastic composite. Mater Des 29:508–513
23. Rawat S, Attia H (2009) Characterization of the dry high speed drilling process of woven composites using machinability maps approach. CIRP Ann-Manuf Technol 58:105–108
24. Rawat S, Attia H (2009) Wear mechanisms and tool life management of WC-Co drills during dry high speed drilling ofwoven carbon fibre composites. Wear 267:1022–1030
25. El-Sonbaty I, Khashaba UA, Machaly T (2004) Factors affecting the machine-ability of GFR/epoxy composites. Compos Struct 63: 329–338
26. Mohan NS, Ramachandra A, Kulkarni SM (2005) Machining of fiber- reinforced thermoplastics: influence of feed and drill size on thrust force and torque during drilling. J Reinforced Plast Compos 24:1247–1257
27. Teti R (2002) Machining of composite materials. CIRP Ann-Manuf Technol 51:611–634
28. Abhishek K, Datta S, Mahapatra SS (2015) Optimization of thrust, torque, entry, and exist delamination factor during drilling of CFRP composites. Int J Adv Manuf Technol 76:401–416
29. Tsao CC (2007) Effect of pilot hole on thrust force by saw drill. Int J Mach Tools Manuf 47:2172–2176
30. Tsao CC (2008) Prediction of thrust force of step drill in drilling composite material by Taguchi method and radial basis function network. Int J Adv Manuf Technol 36:11–18